

Supporting information for:

Suppression of Nanowires clustering in hybrid energy harvesters

*Chengbin Pan¹, Jianchen Hu¹, Enric Grustan-Gutierrez¹, Minh Tuan Hoang², Huiling Duan³,
Julien Yvonnet², Alexander Mitrushchenkov², Gilberte Chambaud², Mario Lanza^{1,*}*

¹Institute of Functional Nano & Soft Materials (FUNSOM), Collaborative Innovation Center of the Ministry of Education, Soochow University, 199 Ren-Ai Road, Suzhou, 215123, China. ²Université Paris-Est, Laboratoire Modélisation et Simulation Multi Echelle, MSME UMR 8208 CNRS, 5 bd Descartes, F-77454 Marne-la-Vallée, France. ³State Key Laboratory for Turbulence and Complex System, Department of Mechanics and Engineering Science, CAPT, College of Engineering, Peking University, Beijing 100871, China.

* Corresponding Author Email: mlanza@suda.edu.cn

Index

Fig. S1. CAFM measurement for a nanowire array containing both single NW and NW clusters.	S-2
Fig. S2. EDX measurement on both top and bottom parts of the optimized sample.	S-2
Fig. S3. Carbon concentration for ten different locations measured at three different optimized samples.	S-3
Fig. S4. Top view of yielded NWs spin-coated with PMMA at 2500 rpm 3 minutes.	S-3
Fig. S5. SEM and CAFM measurement for PMMA-free sample before and after 5 minutes oxygen plasma etching.	S-4
Fig. S6. TEM images of the PMMA-free sample before and after 5 minutes oxygen plasma etching.	S-5
Fig. S7. Detailed top view and cross section of a cluster of four nanowires in the PMMA-free sample.	S-5
Fig. S8. Current maps for the PMMA-free sample using different Pt-Ir varnished AFM tips and deflection setpoint values.	S-6
Fig. S9. An comparison between the current driven by a standard cell and an optimized cell.	S-7
Fig. S10. Morphology and electrical stability characterization by SEM and CAFM.	S-8

The effect of NW clustering on the currents generated is analyzed from current maps. To avoid the sample-to-sample variability, we selected one PMMA-free ZnO nanowire array, which contains both single nanowire (marked by white dashed circles) and nanowire clusters (marked by red dashed circles). The topography and current maps in the absence of light bank (it was fixed at 0%) can be observed in Figures S1 (a) and S1 (b) respectively. We analyze 60 locations of the sample containing (isolated NW, 6 NW clusters, 7 NW clusters, 8 NW clusters) from a series of current maps in this sample. The detailed data is shown in the box chart, as displayed in Figure S1 (c). Interestingly, the current volume generated by a nanowire in the cluster is significantly lower than the one generated by a single nanowire. Furthermore, the current volume generated by per nanowire keeps decreasing for larger clusters.

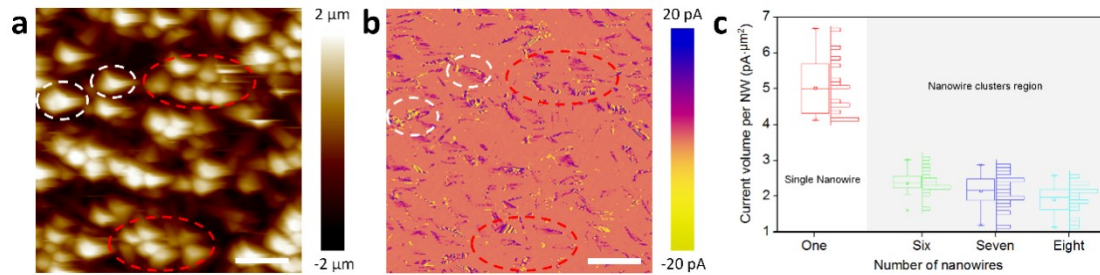


Figure S1: CAFM measurement for a nanowire array which contains both single NW and NW clusters. (a) Topography measurement. (b) Piezo current map. (c) A box chart of the current volume generated by a single nanowire when it is alone or in a NW cluster. The scale bars in panels (a, b) indicate 2 μm.

An EDX measurement was also carried out on both the top and bottom parts of the optimized sample to detect the element difference. As we expected, the carbon element content in the top part is 17.7%, while at the bottom the carbon element signal is significantly enhanced to 28.5%, as shown in Figure S2. This observation corroborates that: i) the PMMA has effectively permeated into the gaps of the NW clusters through the spin-coating; and ii) the PMMA residues in the top part has been effectively removed by the oxygen plasma etching process. More detailed carbon element content information is displayed in Figure S3.

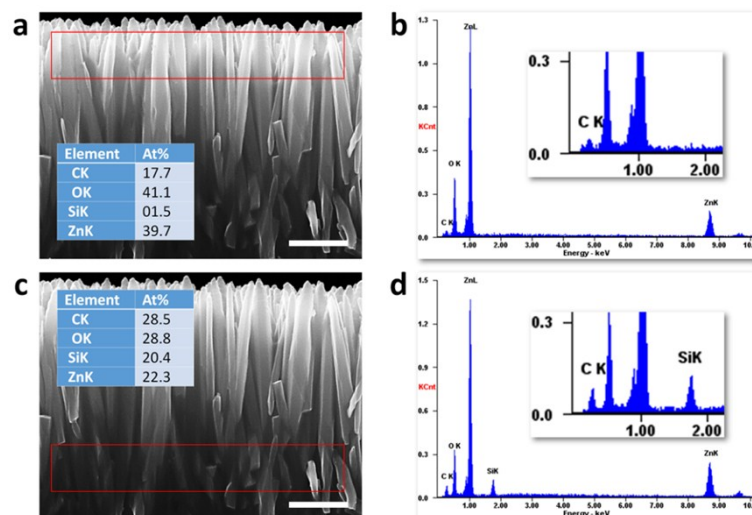


Figure S2: (a, c) SEM images showing where the EDX analyses for a sample spin coated with PMMA and etched during 1.5 minutes. The area under test is highlighted with two red rectangles. (b, d) EDX survey for the top and bottom part of the sample (respectively). The scale bars in panels (a, c) are 1 μm.

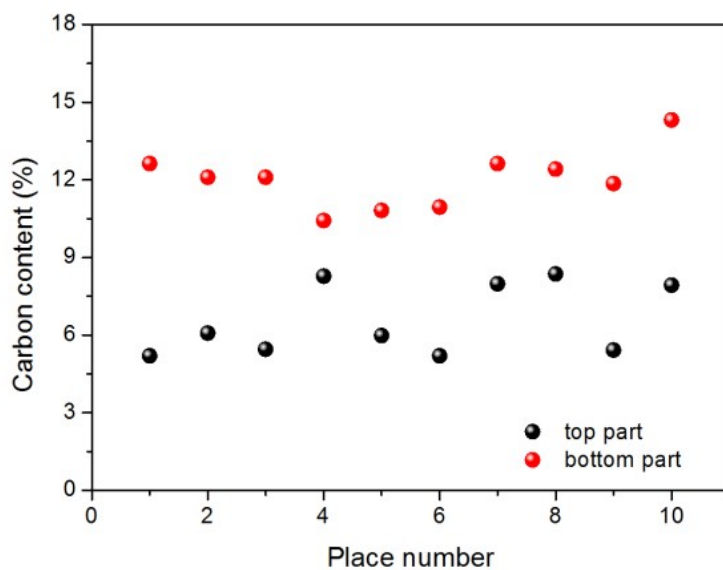


Figure S3: Carbon concentration for ten different locations measured at three different optimized samples. The EDX always shows 1.5 to 3 times more carbon concentration at the bottom part of the nanowires, due to the penetration of PMMA, which is rich in Carbon. Other works also corroborated the presence of carbon from PMMA using EDX [1, 2].

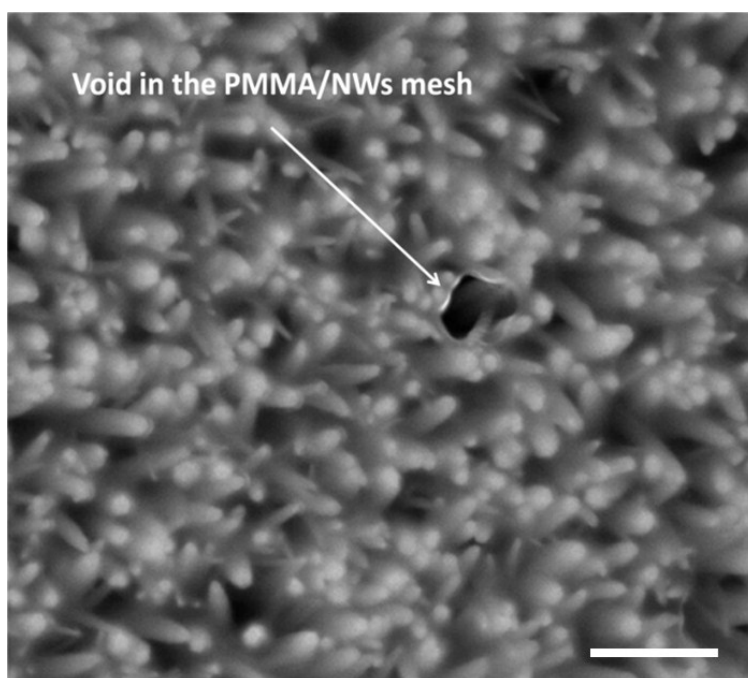


Figure S4: Top view of yielded NWs spin-coated with PMMA at 2500 rpm 3 minutes. A void can be clearly observed, indicating that those spinning parameters are not optimized to form a good PMMA/NWs mesh. The scale bar here indicates 1 μm .

In order to provide more insights into the effect of the oxygen plasma on the NWs, we have scanned the PMMA-free sample with SEM and CAFM before and after 5 minutes oxygen plasma etching (no PMMA has been used in this experiment). Please note that the time used

in this experiment is more than three times larger than that used for the optimized device. The results are presented in Figure S5, and they indicate that both the morphology and currents registered are very similar, indicating that no damage has been induced by the plasma etching process.

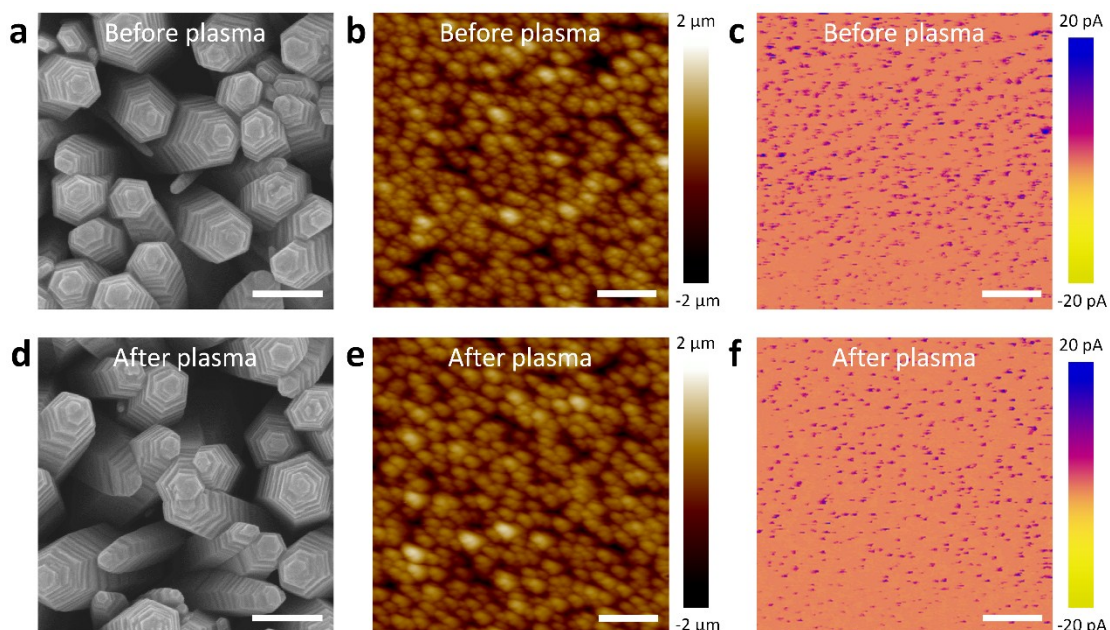


Figure S5: (a, d) SEM images (b, e) topography maps and (c, f) current maps for the PMMA-free sample before and after 5 minutes oxygen plasma etching. The scale bars in panels (a, d) are 1 μm, and in (b, c, e, f) are 2 μm.

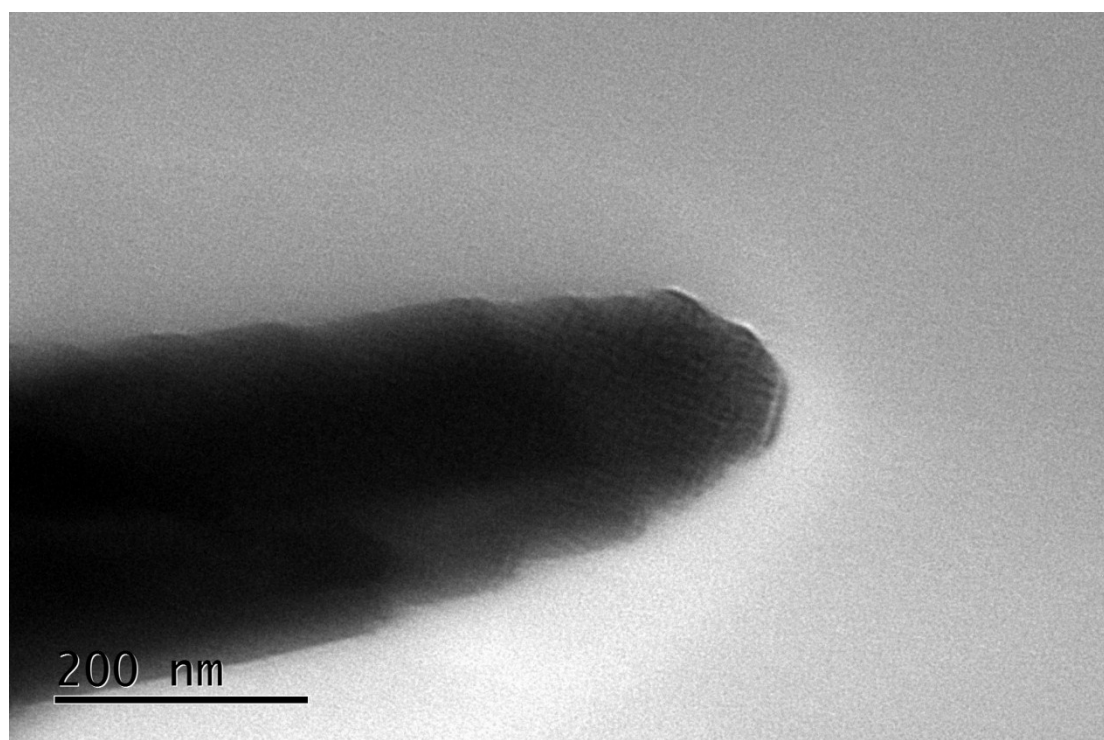


Figure S6: TEM images for the ZnO nanowires after oxygen plasma treatment. The typical stepped surface and crystalline structure reveal near no damage by the plasma.

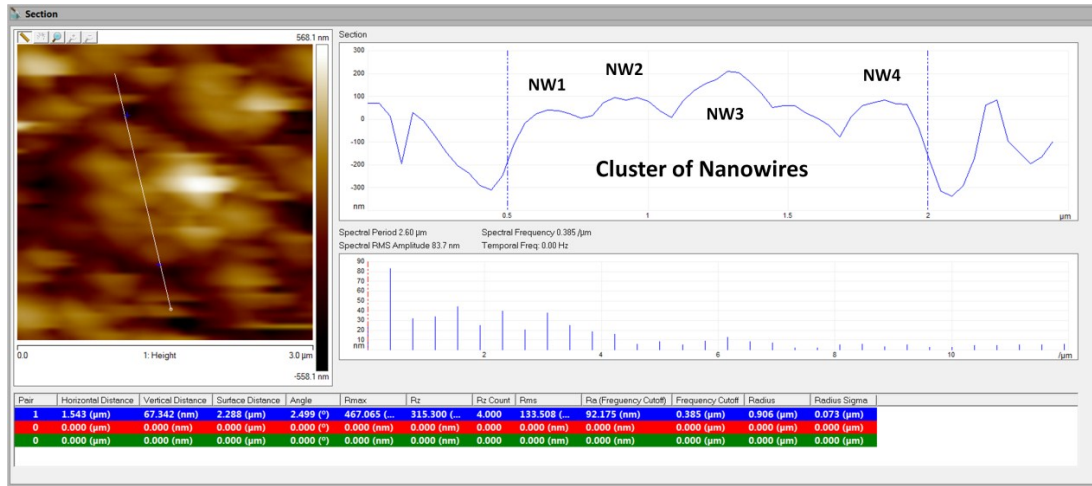


Figure S7: Detailed top view and cross section of a cluster of four nanowires in the PMMA-free sample. The map corresponds to the inset in Figure 2a.

Despite the performance of ZnO NWs based piezoelectric nanogenerators has attracted the attention of many scientists, there is unfortunately no consensus on a procedure to characterize and compare the properties these prototypes. The reason is that there are several factors that influence on the output performance of the cells reported, such as:

- Nanoscale characterization method. For example, professor Z. L. Wang usually characterizes the piezoelectric voltages generated using a CAFM and a load resistor. Other groups (including ourselves) used the currents generated in the CAFM to evaluate the output performance. These two measurements don't allow quantitative comparison of the data, only relative variations are meaningful.
- Contact force exert with the AFM tip. Depending on the deflection setpoint used in the CAFM, and even depending on the spring constant of the cantilever, the mechanical movement induced into the nanowires will be different, which would produce different output currents. Just to show one example, Figure S8 shows the typical CAFM images collected (in the absence of bias) for the PMMA-free sample using two different tips with different properties and under different deflection setpoint value. As it can be observed, the result is completely different.

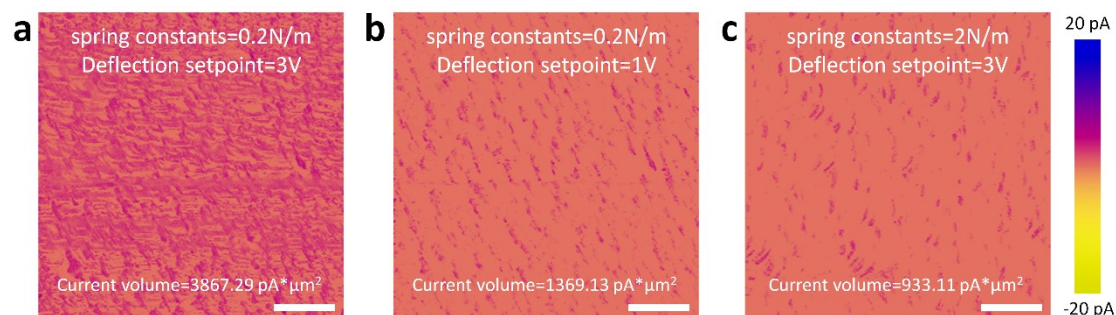


Figure S8: Current map of the PMMA-free sample using Pt-Ir varnished AFM tips with spring constants of (a,b) 0.2 N/m and (c) 2 N/m. (a) and (c) are under the deflection setpoint value of 3V, meanwhile the DS value applied to (b) is 1V. Scale bars here represent 2μm.

- Contact resistance of the tip/sample junction. Another very important parameter is the contact resistance, which will depend on the material and thickness of the metallic varnish of

the tip, as well as its geometry because that will modify the effective tip/sample contact area. Therefore, unless two authors from different groups use the same tip model, quantitative comparisons are not allowed, just relative variations within the results of each group are meaningful.

- Intrinsic deviations. The CAFM is a technique highly sensitive to deviations. For example, two tips from the same box provided by the manufacturer could have different spring constants which, even using the same deflection setpoint, will affect the amount of movement and currents generated by the nanowires.

- Device level and nanoscale setups comparison. It is worth noting that the performances reported at the device level are always much lower than those measured at the nanoscale. To our knowledge, one of the highest performances reported at the device level is $2\mu\text{A}/\text{cm}^2$ for a contact force of 1Kgf [3], and 55mV for 6.25MPa [4]. In our manuscript (as well as in other nanoscale studies), when the AFM tip presses a nanowire exerting a force of 10^{-1}nN on it, since the typical AFM-tip/sample contact area has been reported to be $\sim 100\text{nm}^2$, the pressure being applied is $\sim 10^{-3}\text{nN}/\text{nm}^2$. According to Figure 3, the current density measured for the non-optimized sample is in the order of $\sim 5\text{pA}/100\text{nm}^2$, which equals to $5\text{A}/\text{cm}^2$. Taking into account that the current peaks cover 25% of the total image, the theoretical maximum current in a real device when applying $10^{-3}\text{nN}/\text{nm}^2$ ($\sim 10\text{Kgf}/\text{cm}^2$) is still above $1\text{A}/\text{cm}^2$. This huge difference between performances reported at the nanoscale and device level doesn't allow comparison between works obtained with different setups.

The most suitable figure of merit in the field of nanogenerators would be the power conversion efficiency, given in %. But that is a figure of merit that just a few authors provide in their papers, and never in nanoscale studies. For these reasons, we believe we should be very careful when comparing absolute values from different groups, and generally only relative variations within a paper are correct.

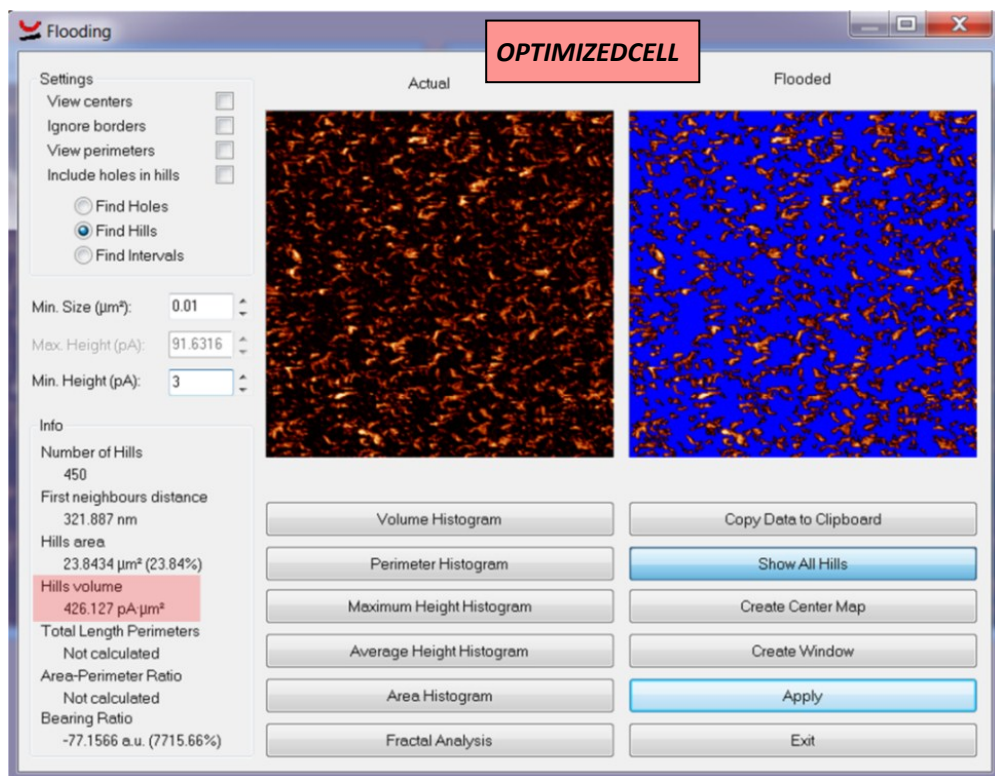
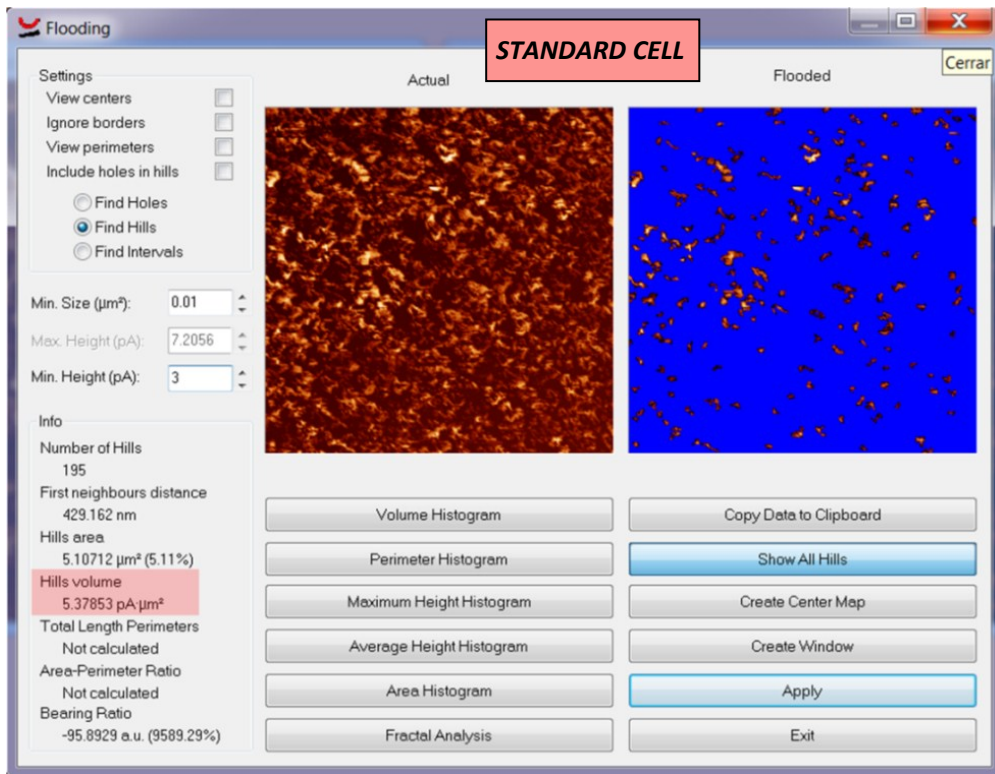


Figure S9: Cell performance increase of the optimized NWs array (spin coated with PMMA at 4000 rpm, and etched in oxygen plasma for 1.5 minutes sample, bottom) compared to the PMMA-free sample (top). Using the same threshold height for both current images (3 pA, called "Min. Height (pA)"), we observe that more current spots are generated in the optimized sample, and they drive larger currents (the "Max. Height (pA)" in the PMMA-free sample is 7.25 pA, while in the optimized sample it is 91.63). This leads to a total current generated ("Hills volume") that is almost 80 times larger for the optimized cell.

As a goal to prove the durability of the morphology and electrical properties of the optimized sample, a sequence of scans have been carried out within 3 months. The results (Figure S10) show good current endurance after several scans. Moreover, the sample has been scanned again 3 months after fabrication. We also provide cross-sectional scanning electron microscope images. Both the current and the morphology look very stable vs. operation and storing time.

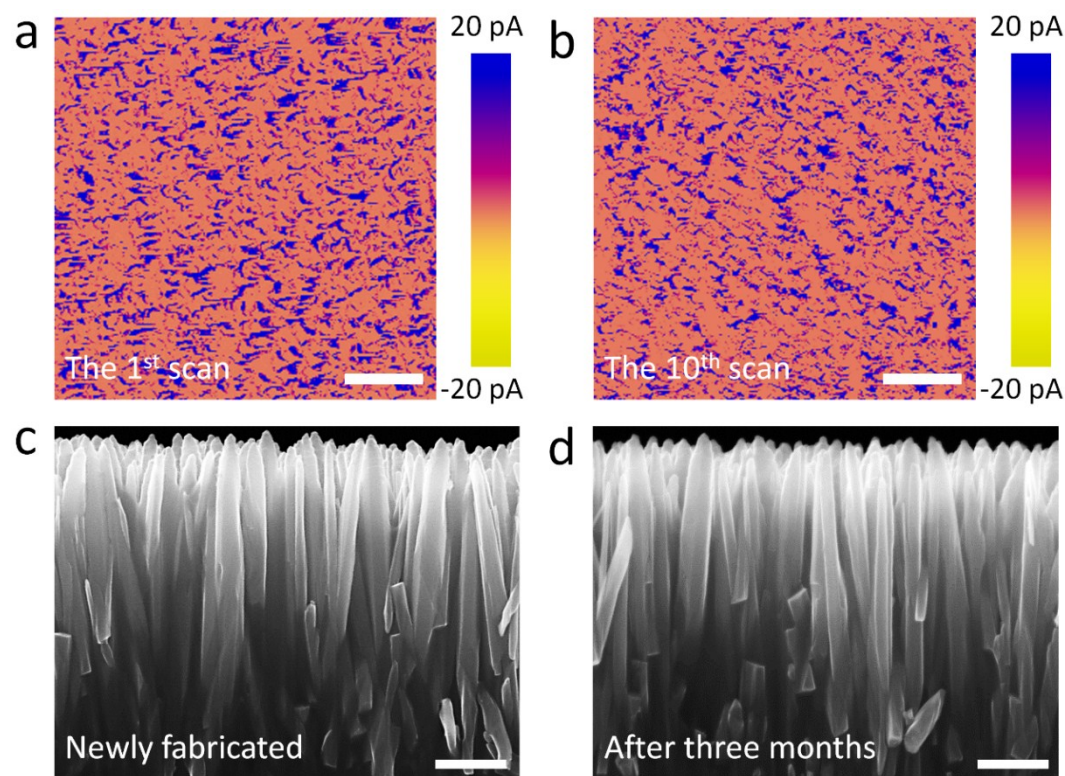


Figure S10: (a, b) Current maps for the same PMMA-penetrated sample at its first and 10th scan respectively. the scale bars in panels (a, b) are 2 μm . (c) SEM images of the new optimized sample. (d) SEM images of the 3-month old optimized sample after scans . The scale bars in panels (c, d) are 1 μm .

ADDITIONAL REFERENCES:

- [1] Lanza, M.; Bayerl, A.; Gao, T.; Porti, M.; Nafria, M.; Jing, G. Y.; Zhang, Y. F.; Liu, Z. F.; Duan, H. L. Graphene-Coated Atomic Force Microscope Tips for Reliable Nanoscale Electrical Characterization. *Adv. Mater.* **2013**, *25*, 1440–1444.
- [2] Sreekanth, T.V.M.; Jung, M. j.; Eom, I. Y. Green Synthesis of Silver Nanoparticles, Decorated on Graphene Oxide Nanosheets and Their Catalytic Activity. *Appl. Surf. Sci.* **2015**, *15*, 02843-3.
- [3] Choi, D.; Choi, M. Y.; Choi, W. M.; Shin, H. J.; Park, H.; Seo, J. S.; Park, J. *Adv. Mater.* **2006**, *22*, 2187 – 2192.
- [4] Xu, S.; Wei, Y.; Liu, L.; Yang, R.; Wang, Z. L. *Nano Lett.* **2011**, *8*, 4027 – 4032.